East European Journal of Physics. 3. 103–115 (2024)
DOI: 10.26565/2312-4334-2024-3-10 ISSN 2312-4334

STUDY ON ANISOTROPIC DARK ENERGY COSMOLOGICAL MODELS IN GENERALIZED BRANS-DICKE THEORY

M. Vijaya Santhi*, **K. SantoshRupa**
Department of Applied Mathematics, Andhra University, Visakhapatnam 530003, India
**Corresponding Author e-mail: gv.santhi@live.com*
Received April 22, 2024; revised June 15, 2024; accepted August 19, 2024

In this present paper, we have investigated the dark energy cosmological model in Bianchi$-VI_0$ spacetime by considering generalised Brans-Dicke theory, self-interacting potential, and a dynamical coupling parameter. For this purpose, we have utilised a hybrid scale factor to approximate the dynamical behaviour of the deceleration parameter. The deceleration parameter should display distinctive flipping behaviour at the transition redshift since the universe is thought to have changed from an early deceleration to a late temporal acceleration. We have studied six alternative transitioning dark energy models on the basis of observational restrictions on the transition redshift. For each model, the behaviour of the dynamical scalar field, the Brans-Dicke parameter, and the self-interacting potential are examined. On top of that, we used the generalised Brans-Dicke theory to estimate how the Newtonian gravitational constant changes over time.

Keywords: *Bianchi type$-VI_0$ metric; Generalized Brans-Dicke theory; Hybrid scale factor; Skewness parameter; Unified dark fluid*

PACS: 95.36+X, 98.80-k, 95.30-sf

1. INTRODUCTION

The recent observations of the universe's accelerated expansion were supported by Riess et al. [1] and Perlmutter et al. [2] through various observational facts. The universe appears to be spatially flat and dominated by dark energy, an exotic substance with high negative pressure, according to cosmological measurements and data from the cosmic microwave background [3, 4]. Additionally, it is hypothesised that dark energy makes up 68.3% of the energy in our universe, dark matter 26.8%, and baryonic matter 4.9% [5, 6]. Two methods have been put forth to explain this late-time acceleration: one is to develop different dark energy candidates, and the other is to alter Einstein's gravitational theory. Developed in 1916, Einstein's general theory of relativity offered a sophisticated description of gravitation. It has done a fantastic job of characterising gravitational phenomena. Models of the cosmos have also been built on top of it. The homogeneous isotropic expanding model based on general relativity seems to give a decent approximation to the observed large-scale features of the cosmos. In recent years, there have been some intriguing attempts to generalise general relativity by including Mach's principle and other desirable aspects that the original theory lacks, for example, general relativity does not fully account for the inertial properties of matter. Modified gravity theories of general relativity (GR) have long been a hot area for research. The Brans-Dicke (BD) theory [7] is a simple scalar tensor extension of general relativity (GR) in which a dynamical scalar field is non-minimally connected to curvature. As a result, the Newtonian constant G becomes inversely proportional to the scalar field ϕ and hence a function of coordinates. The departure of the results obtained in this theory under weak field approximation from those found in general relativity under similar approximation is determined by a dimensionless parameter $\mathcal{W}$, dubbed the Brans-Dicke coupling parameter. The lower the value of $\mathcal{W}$, the more disparate the related outcomes. General relativity is well recognized for explaining local astronomical tests very effectively, and the value of $\mathcal{W}$ needed for BD theory to be consistent with such observations is too high ($\mathcal{W} > 500$), making BD theory nearly identical to GR in the weak field limit [8]. For numerous reasons, BD theory has a periodic renaissance, particularly in cosmology. For instance, the extended inflation suggested by BD theory [9, 10] helped remove the gracious exit issue associated with traditional inflationary models. In more recent years, the BD hypothesis has been employed to perfect the environment for the universe's late temporal acceleration [**?**, 11, 12, 14, 15]. The amazing aspect is that, on its own, BD theory can produce an accelerated expansion without the aid of any exotic fields by simply selecting an appropriate value for the parameter $\mathcal{W}$ [16].

The current study examines a generalized BD(GBD) theory where the parameter is a function of the scalar field inside the framework established by Nordtvedt [17]. The presence of a potential $\mathcal{V} = \mathcal{V}(\phi)$ is also included in our study as a generalization. The stability criteria were discovered to differ as expected. Mimoso and Nunes [18] worked on a BD theory generalization with either radiation or a cosmological constant as the matter content. They worked in a conformally altered version of the theory where the action resembled that of a minimally coupled theory and discovered that GR is an attractor of the BD theory. The conformally converted version has the disadvantage that the concept of equivalence is no longer applicable because the rest mass of the test particles becomes a function of the BD scalar field. The study of the

Cite as: M.V. Santhi, K.S. Rupa, East Eur. J. Phys. 3, 103 (2024), https://doi.org/10.26565/2312-4334-2024-3-10

potential impacts of anisotropy in the early universe is greatly aided by spatially homogenous and anisotropic Bianchi−type cosmological models in the presence of scalar forces.

In order to paint a realistic image of the cosmos in its infancy, a wide range of spatially homogeneous and anisotropic cosmological models have been extensively researched within the framework of general relativity. Numerous writers have examined GR-based cosmological models, scalar tensor models, and modified theories. Bianchi type$-VI_0$ space time in BD theory has been examined by Santhi et al [19]. Hegazy and Rahaman [20] talked about the general theory of relativity's Bianchi type$-VI_0$ cosmological model, which has a variable deceleration parameter and an electromagnetic field. The anisotropic Bianchi type$-VI_0$ cosmological model with massive scalar field and dark energy fluid was investigated dynamically by Aditya et al [21]. The magnetized Bianchi Type$-VI_0$ string cosmological model for anti-stiff fluids in general relativity was studied by Chhajed et al [22]. Tripathy et al [23]. examined unified dark fluid and cosmic transit models in Brans-Dicke theory.

Inspired by all the above researchers, we take into account Bianchi type$-VI_0$ space time filled with anisotropic dark energy in the GBD theory with a self-interacting potential. Here we created various dark energy models with a hallmark flipping behaviour of the cosmos from early slowdown to late time acceleration in the framework of generalized BD theory. The organisation of this article is as follows. In section 2, we derived all the mathematical formations of the metric that is considered. Section 3 discussed the dark fluid model and section 4 is devoted to the study of the certain properties. In the subsequent sections, various discussions will be made regarding flipping nature, the Brans-Dicke parameter, the self-interacting potential, and the gravitational constant. In the final section, we have mentioned conclusions on the current study.

2. STRUCTURE OF THE METRIC AND THE MODEL

We consider the homogeneous and anisotropic space-time represented by the Bianchi type-VI_0 metric as

$$ds^2 = -dt^2 + \mathcal{A}^2(t)dx^2 + e^{2a_1x}\mathcal{B}^2(t)dy^2 + e^{-2a_1x}\mathcal{C}^2(t)dz^2 \ , \tag{1}$$

where a_1 is a constant that is not zero and the scale factors $\mathcal{A}$, $\mathcal{B}$, and C are purely functions of cosmic time t.

Here, we take into account the self-interacting potential of the GBD hypothesis. The BD parameter is regarded as a function of the scalar field ϕ, which mediates gravity through a dynamical scalar field. In a Jordan frame, the GBD theory's action is provided by

$$S = \int d^4x\sqrt{-g}\left[\phi R - \frac{\mathcal{W}(\phi)}{\phi}\phi^{,i}\phi_{,i} - \mathcal{V}(\phi) + \mathcal{L}_m\right], \tag{2}$$

where R is the scalar curvature, $\mathcal{W}(\phi)$ is the modified BD parameter, $\mathcal{V}(\phi)$ is the self-interacting potential, and $\mathcal{L}_m$ is the matter Lagrangian.

The GBD theory's field equations are derived as ,

$$R_{ij} - \frac{1}{2}g_{ij}R = \frac{8\pi}{\phi}T_{ij} - \frac{\mathcal{W}(\phi)}{\phi^2}\left[\phi_i\phi_j - \frac{1}{2}g_{ij}\phi_{,\alpha}\phi^{,\alpha}\right] - \frac{1}{\phi}\left[\phi_{,i;j} - g_{ij}\Box\phi\right], \tag{3}$$

where

$$\Box\phi = \frac{T}{2\mathcal{W}(\phi)+3} - \frac{2\mathcal{V}(\phi) - \phi\frac{\partial\mathcal{V}(\phi)}{\partial\phi}}{2\mathcal{W}(\phi)+3} - \frac{\frac{\partial\mathcal{W}(\phi)}{\partial\phi}\phi_{,i}\phi^{,i}}{2\mathcal{W}(\phi)+3}. \tag{4}$$

The energy momentum tensor's trace is represented by $T = g^{ij}T_{ij}$ in the equations above, where $\Box$ is the D'Alembert operator.

The definition of the anisotropic fluid's energy-momentum tensor is

$$T^i_j = diag(-\rho, P_x, P_y, P_z) \quad , \tag{5}$$

where p_x, p_y and p_z are the pressures; ρ is the energy density;
Additionally, the energy conservation equation serves as

$$(T^{ij})_{;j} = 0.$$

With the aid of the energy momentum tensor, the GBD theory field equations for the metric (1) are

$$\frac{\ddot{\mathcal{B}}}{\mathcal{B}} + \frac{\ddot{C}}{C} + \frac{\dot{\mathcal{B}}\dot{C}}{\mathcal{B}C} + \frac{a_1^2}{\mathcal{A}^2} + \frac{\mathcal{W}}{2}\frac{\dot{\phi}^2}{\phi^2} + \left(\frac{\dot{\mathcal{B}}}{\mathcal{B}} + \frac{\dot{C}}{C}\right)\frac{\dot{\phi}}{\phi} + \frac{\ddot{\phi}}{\phi} = \frac{8\pi p}{\phi} + \frac{\mathcal{V}(\phi)}{2\phi}, \tag{6}$$

$$\frac{\ddot{\mathcal{A}}}{\mathcal{A}} + \frac{\ddot{C}}{C} + \frac{\dot{\mathcal{A}}\dot{C}}{\mathcal{A}C} - \frac{a_1^2}{\mathcal{A}^2} + \frac{\mathcal{W}}{2}\frac{\dot{\phi}^2}{\phi^2} + \left(\frac{\dot{\mathcal{A}}}{\mathcal{A}} + \frac{\dot{C}}{C}\right)\frac{\dot{\phi}}{\phi} + \frac{\ddot{\phi}}{\phi} = \frac{8\pi p}{\phi} + \frac{\mathcal{V}(\phi)}{2\phi} \ , \tag{7}$$

$$\frac{\ddot{\mathcal{A}}}{\mathcal{A}}+\frac{\ddot{\mathcal{B}}}{\mathcal{B}}+\frac{\dot{\mathcal{A}}\dot{\mathcal{B}}}{\mathcal{A}\mathcal{B}}-\frac{a_1^2}{\mathcal{A}^2}+\frac{\mathcal{W}}{2}\frac{\dot{\phi}^2}{\phi^2}+\left(\frac{\dot{\mathcal{A}}}{\mathcal{A}}+\frac{\dot{\mathcal{B}}}{\mathcal{B}}\right)\frac{\dot{\phi}}{\phi}+\frac{\ddot{\phi}}{\phi}=\frac{8\pi p}{\phi}+\frac{\mathcal{V}(\phi)}{2\phi}, \tag{8}$$

$$\frac{\dot{\mathcal{A}}\dot{\mathcal{B}}}{\mathcal{A}\mathcal{B}}+\frac{\dot{\mathcal{B}}\dot{\mathcal{C}}}{\mathcal{B}\mathcal{C}}+\frac{\dot{\mathcal{A}}\dot{\mathcal{C}}}{\mathcal{A}\mathcal{C}}-\frac{a_1^2}{\mathcal{A}^2}-\frac{\mathcal{W}}{2}\frac{\dot{\phi}^2}{\phi^2}+\left(\frac{\dot{\mathcal{A}}}{\mathcal{A}}+\frac{\dot{\mathcal{B}}}{\mathcal{B}}+\frac{\dot{\mathcal{C}}}{\mathcal{C}}\right)\frac{\dot{\phi}}{\phi}=-\frac{8\pi\rho}{\phi}+\frac{\mathcal{V}(\phi)}{2\phi}, \tag{9}$$

$$\frac{\dot{\mathcal{B}}}{\mathcal{B}}-\frac{\dot{\mathcal{C}}}{\mathcal{C}}=0, \tag{10}$$

and

$$\ddot{\phi}+\dot{\phi}\left(\frac{\dot{\mathcal{A}}}{\mathcal{A}}+\frac{\dot{\mathcal{B}}}{\mathcal{B}}+\frac{\dot{\mathcal{C}}}{\mathcal{C}}\right)=\frac{\rho-3p}{2\mathcal{W}(\phi)+3}+\frac{2\mathcal{V}(\phi)-\phi\frac{\partial\mathcal{V}(\phi)}{\partial\phi}}{2\mathcal{W}(\phi)+3}-\frac{\frac{\partial\mathcal{W}(\phi)}{\partial\phi}\dot{\phi}^2}{2\mathcal{W}(\phi)+3}. \tag{11}$$

From the above set of equations , we obtain

$$\frac{2\ddot{\mathcal{B}}}{\mathcal{B}}+\frac{\dot{\mathcal{B}}^2}{\mathcal{B}^2}+\frac{a_1^2}{\mathcal{A}^2}+\frac{\mathcal{W}}{2}\frac{\dot{\phi}^2}{\phi^2}+(\frac{2\dot{\mathcal{B}}}{\mathcal{B}})\frac{\dot{\phi}}{\phi}+\frac{\ddot{\phi}}{\phi}=\frac{8\pi p}{\phi}+\frac{\mathcal{V}(\phi)}{2\phi}, \tag{12}$$

$$\frac{\ddot{\mathcal{A}}}{\mathcal{A}}+\frac{\ddot{\mathcal{B}}}{\mathcal{B}}+\frac{\dot{\mathcal{A}}\dot{\mathcal{B}}}{\mathcal{A}\mathcal{B}}-\frac{a_1^2}{\mathcal{A}^2}+\frac{\mathcal{W}}{2}\frac{\dot{\phi}^2}{\phi^2}+\left(\frac{\dot{\mathcal{A}}}{\mathcal{A}}+\frac{\dot{\mathcal{B}}}{\mathcal{B}}\right)\frac{\dot{\phi}}{\phi}+\frac{\ddot{\phi}}{\phi}=\frac{8\pi p}{\phi}+\frac{\mathcal{V}(\phi)}{2\phi}, \tag{13}$$

$$\frac{2\dot{\mathcal{A}}\dot{\mathcal{B}}}{\mathcal{A}\mathcal{B}}+\frac{\dot{\mathcal{B}}^2}{\mathcal{B}^2}+\frac{\dot{\mathcal{A}}\dot{\mathcal{B}}}{\mathcal{A}\mathcal{B}}-\frac{a_1^2}{\mathcal{A}^2}-\frac{\mathcal{W}}{2}\frac{\dot{\phi}^2}{\phi^2}+\left(\frac{\dot{\mathcal{A}}}{\mathcal{A}}+\frac{2\dot{\mathcal{B}}}{\mathcal{B}}\right)\frac{\dot{\phi}}{\phi}=-\frac{8\pi\rho}{\phi}+\frac{\mathcal{V}(\phi)}{2\phi}, \tag{14}$$

and

$$\ddot{\phi}+\dot{\phi}\left(\frac{\dot{\mathcal{A}}}{\mathcal{A}}+\frac{2\dot{\mathcal{B}}}{\mathcal{B}}\right)=\frac{\rho-3p}{2\mathcal{W}(\phi)+3}+\frac{2\mathcal{V}(\phi)-\phi\frac{\partial\mathcal{V}(\phi)}{\partial\phi}}{2\mathcal{W}(\phi)+3}-\frac{\frac{\partial\mathcal{W}(\phi)}{\partial\phi}\dot{\phi}^2}{2\mathcal{W}(\phi)+3}. \tag{15}$$

Where the overhead dot stands for ordinary differentiation with respect to t.

Solving equation(10), we obtain

$$\mathcal{C}=m\mathcal{B} \tag{16}$$

The field equations (12) − (15) are now a system of four independent equations with eight unknown parameters ($\mathcal{A}$, $\mathcal{B}$, p, ρ, ϕ, δ_y, $\mathcal{V}(\phi)$ and $\mathcal{W}(\phi)$). To obtain a determinate solution to the field equations, we consider the following suitable conditions, which are physically viable.

i) We assume that the expansion scalar (θ) is proportional to the shear scalar (σ) from [25]. This condition leads to ,

$$\mathcal{A}=\mathcal{B}^n, \tag{17}$$

where n≠1 is a constant.

ii) By the motivation of Tripathy et. al. [23], we take a look at a hybrid scale factor(HSF),

$$a(t)=a_0\left(\frac{t}{t_0}\right)^{\mathcal{H}^1}e^{\mathcal{H}^0(t-t_0)}, \tag{18}$$

where a_0 is the scale factor at the current epoch t_0 and $\mathcal{H}^0$ and $\mathcal{H}^1$ are HSF parameters whose values are positive constants, and in this work, we have assumed $a_0=t_0=1$.
Spatial volume of the model and average scale factor are given by

$$V=\sqrt{-g}\qquad and\qquad a(t)=V^{1/3}.$$

Then we obtain,

$$\mathcal{A}=\frac{1}{m^{\frac{n}{(n+2)}}}t^{\frac{3\mathcal{H}^1 n}{(n+2)}}e^{\frac{3\mathcal{H}^0 n(t-1)}{n+2}}, \tag{19}$$

$$\mathcal{B}=\frac{1}{m^{\frac{1}{(n+2)}}}t^{\frac{3\mathcal{H}^1}{(n+2)}}e^{\frac{3\mathcal{H}^0(t-1)}{n+2}}, \tag{20}$$

and

$$\mathcal{C}=\frac{1}{m^{\frac{1}{(n+2)}-1}}t^{\frac{3\mathcal{H}^1}{(n+2)}}e^{\frac{3\mathcal{H}^0(t-1)}{n+2}}. \tag{21}$$

From equations (12) and (13), we get

$$\frac{\dot{\mathcal{A}}}{\mathcal{A}} - \frac{\dot{\mathcal{B}}}{\mathcal{B}} = \frac{c_1}{\mathcal{A}\mathcal{B}^2\phi} e^{\int \left(\frac{\frac{2a_1^2}{\mathcal{A}^2}}{\frac{\dot{\mathcal{A}}}{\mathcal{A}} - \frac{\dot{\mathcal{B}}}{\mathcal{B}}} \right) dt}, \tag{22}$$

where c_1 is an integral constant.

Assume

$$\delta_0 = e^{\int \left(\frac{\frac{2a_1^2}{\mathcal{A}^2}}{\frac{\dot{\mathcal{A}}}{\mathcal{A}} - \frac{\dot{\mathcal{B}}}{\mathcal{B}}} \right) dt}. \tag{23}$$

From equations (19)– (23) , we get,

$$\frac{\phi}{\phi_0} = t^{-3\mathcal{H}^1} e^{-3\mathcal{H}^0(t-1)} \left(\frac{\mathcal{H}^1}{t} + \mathcal{H}^0 \right)^{-1}, \tag{24}$$

where $\phi_0 = \frac{m\, c_1\, \delta_0\, (n+2)}{3(n-1)}$.

The field equations (12) through (15) are used to get the Brans-Dicke parameter and the self-interacting potential, as

$$\mathcal{W}(\phi) = \left[-3\frac{(\mathcal{H}^1 + \mathcal{H}^0 t)}{t} + \frac{\mathcal{H}^1}{t(\mathcal{H}^1 + \mathcal{H}^0 t)} \right]^{-2} \left\{ \begin{array}{l} \dfrac{8\pi(\rho + p)}{\phi_0 t^{-3\mathcal{H}^1} e^{-3\mathcal{H}^0(t-1)} \left(\frac{\mathcal{H}^1}{t} + \mathcal{H}^0 \right)^{-1}} - \dfrac{9(2n^2 + 3n + 5)(\mathcal{H}^1 + \mathcal{H}^0 t)^2}{(n+2)^2 t^2} \\ - 2\left(\dfrac{\mathcal{H}^1}{t(\mathcal{H}^1 + \mathcal{H}^0 t)} \right)^2 \end{array} \right\}, \tag{25}$$

and

$$\mathcal{V}(\phi) = \left[\phi_0 t^{-3\mathcal{H}^1} e^{-3\mathcal{H}^0(t-1)} \left(\frac{\mathcal{H}^1}{t} + \mathcal{H}^0 \right)^{-1} \right] \left\{ \begin{array}{l} -3(n+5)\dfrac{\mathcal{H}^1}{t^2} + \dfrac{9(n^2 + 7n + 2)}{(n+2)^2} \left(\dfrac{\mathcal{H}^1}{t} + \mathcal{H}^0 \right)^2 \\ + \dfrac{2(\mathcal{H}^1)^2}{t^2(\mathcal{H}^1 + \mathcal{H}^0 t)^2} - \dfrac{2\mathcal{H}^1}{t^2(\mathcal{H}^1 + \mathcal{H}^0 t)} \end{array} \right\} + 8\pi(\rho - p) \ , \tag{26}$$

Here, in order to determine the dynamical BD parameter and the self-interacting potential, we take into consideration a straightforward linear equation of state known as the equation of state of the unified dark fluid (UDF). Dark energy and dark matter, which are two separate concepts, are how the UDF explains how both dark sectors can come together. It is important to note here that there are several generalized equations of states in the literature that consider dark energy and dark matter as two different sides of the same cosmic fluid [26].

3. UNIFIED DARK FLUID

Undisputedly, exotic dark energy and non-baryonic matter are the main drivers of late-time cosmic acceleration. Recent Planck measurements show that the universe's mass-energy budget is made up of 68.3% dark energy, 26.8% dark matter and 4.9% baryonic matter and that the dark sector, which comprises dark energy and dark matter, accounts for about 95% of that budget. The mysterious cosmic speed-up phenomenon in the late hours has several possible causes. Various theories and notions have been created to better understand the phenomenon. This could be accomplished by using a particular strategy that unifies dark energy and dark matter into a single UDF. After the generalized Chaplygin gas model (CGM) was successful in addressing concerns about the late-time cosmic acceleration and dark energy problem [27], a dark fluid model with a linear equation of state

$$p = \alpha\,(\rho - \rho_0)\,, \tag{27}$$

was presented. Here, the UDF's constant parameters α and ρ_0 are used. The adiabatic sound speed of the UDF is constant, $C_s^2 = \frac{dp}{d\rho} = \alpha$. Both hydrodynamically stable ($\alpha > 0$) and unstable ($\alpha < 0$) fluids are described by this non-homogeneous linear equation of state. The conservation equation is

$$\dot{\rho} + 3H(P + \rho) = 0, \tag{28}$$

by integrating equation (28),

$$\rho = \frac{\alpha}{(1+\alpha)}\rho_0 + \frac{c_2}{(1+\alpha)} \frac{1}{t^{3\mathcal{H}^1(1+\alpha)} e^{3\mathcal{H}^0 t(1+\alpha)}}, \tag{29}$$

where c_2 is an integrating constant.
From equations (27) and (29), we derive

$$p = \frac{-\alpha}{(1+\alpha)}\rho_0 + \frac{c_2\alpha}{(1+\alpha)}\frac{1}{t^{3\mathcal{H}^1(1+\alpha)}e^{3\mathcal{H}^0 t(1+\alpha)}}\ , \tag{30}$$

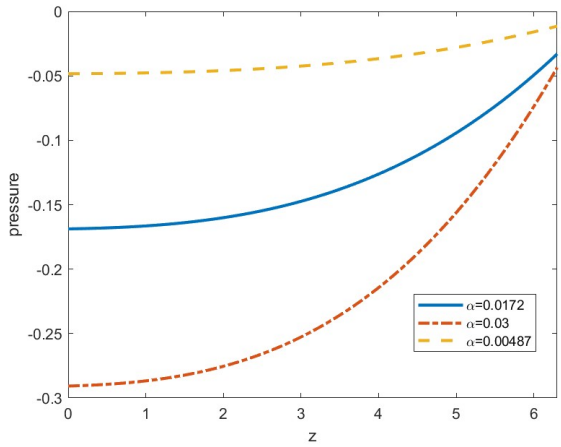

Figure 1. Study of pressure over the redshift parameter

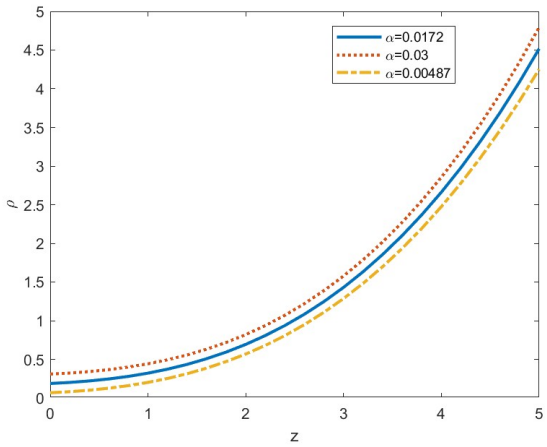

Figure 2. Analysis of density in terms of redshift parameter

The dark energy equation of state can be seized as the following when considering the redshift:

$$\omega_D = \frac{p}{\rho} = \alpha - \frac{\alpha(1+\alpha)\rho_0}{\left(\alpha\rho_0 + c^1 e^{-3\mathcal{H}^0(1+\alpha)}(1+z)^{3(1+\alpha)}\right)}\ , \tag{31}$$

where we have used the fact $1 + z = \frac{1}{a}$.

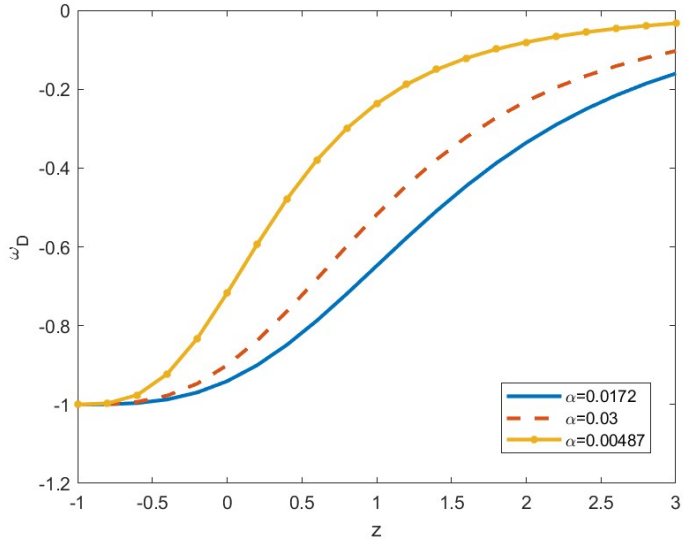

Figure 3. For three different values of α, the dark energy equation of state in terms of red shift.

Figure (3) depicts the dark energy equation of the state's evolutionary behaviour for three different values of the limited adiabatic sound speed α The dynamical behavior of a bouncing model has been discussed in the framework of the dark energy equation of state for UDF. Here, we fixed the values for constants $\mathcal{H}^0 = 0.55, c_2 = 0.1, \rho_0 = 10$ using various values of constants. A change in these values, as observed in this work, does not effect on ω_D's overall dynamical behaviour. In light of this, we used $\mathcal{H}^0 = 0.55, c_2 = 0.1, \rho_0 = 10$ to plot the figure in the current work. According to the illustration, the lower curve in the graphic reflects the value $\alpha = 0.0172$, the middle curve to the value $\alpha = 0.03$ and the higher curve to the value $\alpha = 0.00487$. Depending on various conditions, the dark energy equation of state can change in

a variety of ways. Consequently, affects the slope of ω_D. Regardless of the value of α, ω_D eventually develops to overlap with the ΛCDM model ($\omega_D = -1$).

3.1. Unified dark fluid in $\omega'_D - \omega_D$

In order to evaluate the quintessence scalar field, Caldwell and Linder [29,30] first developed the EoS plane to explain the areas of the expanding Universe. Two unique zones are characterised by the plane for varying values of ω_D and ω'_D. When $\omega'_D > 0$, $\omega_D < 0$, the plane is referred to as a thawing region and when $\omega'_D < 0$, $\omega_D < 0$, it is a freezing region. ω'_D is obtained for this model is,

$$\omega'_D = \frac{-3\alpha(1+\alpha)^2 c^1 t^{-3\mathcal{H}^1(1+\alpha)} e^{-3\mathcal{H}^0 t(1+\alpha)\left(\frac{\mathcal{H}^1}{t}+\mathcal{H}^0\right)}}{\left[\alpha\rho_0 + c^1 t^{-3\mathcal{H}^1(1+\alpha)} e^{-3\mathcal{H}^0 t(1+\alpha)}\right]}. \tag{32}$$

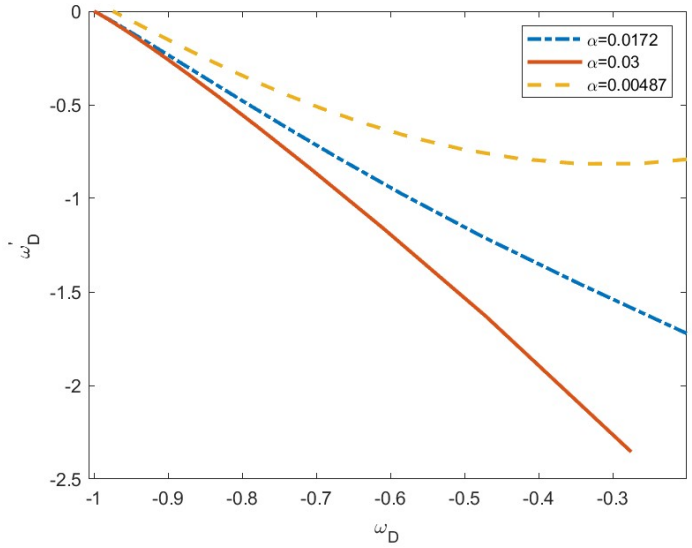

Figure 4. Overview of ω'_D against ω_D

The EoS plane ($\omega'_D - \omega_D$) for this cosmological model is shown in Figure (4) for various values of $\alpha = 0.0172$, $\alpha = 0.3$ and $\alpha = 0.00487$. As $\omega'_D < 0$, $\omega_D < 0$ for our model, it is seen that the model is in the freezing area. This shows that the universe is expanding faster than before.

4. PARAMETERS OF THE MODEL

- **Hubble Parameter:** Hubble's parameter is

$$H = \frac{\dot{\mathcal{A}}}{\mathcal{A}} + 2\frac{\dot{\mathcal{B}}}{\mathcal{B}} = \frac{\mathcal{H}^1}{t} + \mathcal{H}^0. \tag{33}$$

- **Expansion scalar:**

$$\theta = 3H = 3\left[\frac{\mathcal{H}^1}{t} + \mathcal{H}^0\right]. \tag{34}$$

- **Shear scalar:**

$$\sigma^2 = \frac{1}{2}\left(\sum_{i=1}^{3} H_i{}^2 - \frac{\theta^2}{3}\right) = \frac{(n-1)^2}{(n+2)^2}\left(\frac{\mathcal{H}^1}{t} + \mathcal{H}^0\right)^2. \tag{35}$$

- **Anisotropic parameter:**

$$A_h = \frac{1}{3}\sum_{i=1}^{3}\left(\frac{H_i - H}{H}\right)^2 = \frac{6(n^2+2n+3)}{(n+2)^2}. \tag{36}$$

- **State-finder parameters:**

$$r = \frac{\ddot{a}}{aH^3} = \frac{1}{(\frac{\mathcal{H}^1}{t} + \mathcal{H}^0)^3}\left[\frac{\mathcal{H}^1(\mathcal{H}^1-1)(H^2-2)}{t^3} + \frac{3\mathcal{H}^1\mathcal{H}^0(\mathcal{H}^1-1)}{t^2} + \frac{3\mathcal{H}^1\mathcal{H}^0}{t} + (\mathcal{H}^0)^3\right], \tag{37}$$

and

$$s = \frac{r-1}{3(q-\frac{1}{2})} = \frac{4\mathcal{H}^1}{(\mathcal{H}^1+\mathcal{H}^0 t)(2\mathcal{H}^1 - 3(\mathcal{H}^1+\mathcal{H}^0 t)^2)} - \frac{6\mathcal{H}^1}{(2\mathcal{H}^1 - 3(\mathcal{H}^1+\mathcal{H}^0 t)^2)}. \tag{38}$$

- **Deceleration parameter:** The scale-factor $a(t)$ yields the following expression for the deceleration parameter $q(z)$:

$$q = \frac{-a\ddot{a}}{\dot{a}^2} = -1 + \frac{\mathcal{H}^1}{(\mathcal{H}^1+\mathcal{H}^0 t)^2}. \tag{39}$$

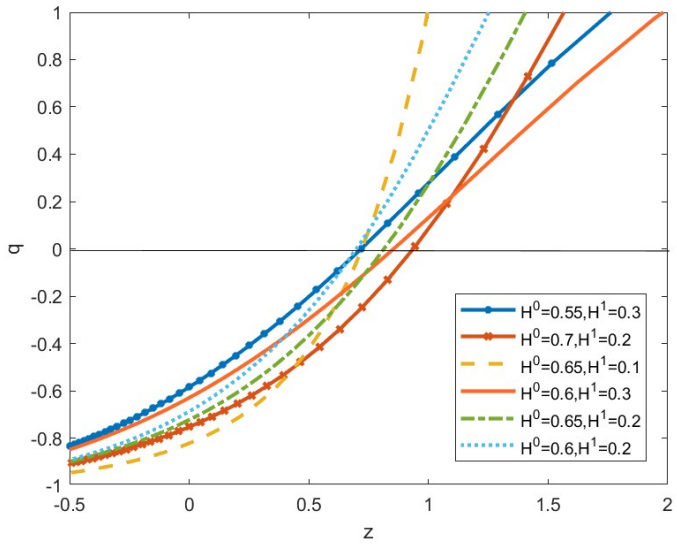

Figure 5. Study of deceleration parameter over z for various values of $\mathcal{H}^0$ and $\mathcal{H}^1$

The fluctuation of DP for the different sets of the HSF model parameters is shown in Figure (5). As illustrated in Table 1, we can see that $q(z)$ is an increasing function of redshift z and exhibits a signature-flipping (transition) point at z_a within the range $0.65 < z_a < 0.9$, where $q(z_a) = 0$ and $q(z) < 0$ for $z < z_a$ and $q(z) > 0$ for $z > z_a$, as well as $q(z) \longleftrightarrow -1$ as $z \longleftrightarrow -1$ and $q(z)$ tends to a finite positive value as $z \longrightarrow \infty$.
Our universe is accelerating right now and decelerating in the early phases, which are quite close to the most recent observations, based on the behaviour of DP $q(z)$ over redshift z. As a result, in line with the most recent research evidence, our model's derivation depicts a transit phase from a universe that is slowing down to one that is accelerating.

5. FLIPPING NATURE

Observations in the past indicate that the universe is growing more rapidly now than in earlier epochs. The idea that the cosmos may have changed from a decelerating to an accelerating phase is also held. The cosmic redshift at which this transition takes place is known as the transition redshift z_a . Inversion of the signature is implied.

The q's behaviour shifts from a positive value early in cosmic evolution to a negative value later. In the current work, we seek to construct a cosmological model that can both forecast how this universe will behave and offer a distinctive flipping of the deceleration parameter. Taking into account a hybrid scale factor equation (18).

This hybrid scale factor consists of two parts, one of which expands exponentially and the other of which expands power law-like. At the beginning of cosmic evolution, power law behaviour rules over cosmic dynamics, in contrast to the exponential factor's supremacy at the end. The exponential law is recovered when $\mathcal{H}^1 = 0$, and a power law expansion is simulated by the scaling factor when $\mathcal{H}^0 = 0$. Power law and the exponential rule of expansion were previously employed by Tripathy et al. [24] to construct certain UDF models within the context of GBD theory. Both the power law and the exponential law of expansion produce a constant deceleration parameter. We suggest utilising a hybrid expansion law in which the deceleration parameter changes from positive to negative values early in cosmic history on account of

the behaviour of planetary transit. The deceleration parameter for this model is $q = -1 + \frac{\mathcal{H}^1}{\left(\mathcal{H}^0 t + \mathcal{H}^1\right)^2}$, while the Hubble parameter is $H = \mathcal{H}^0 + \frac{\mathcal{H}^1}{t}$. Mishra and Tripathy [31–36], in their recent publications, have addressed a number of issues relating to the late-time cosmic speed-up event within the context of GR and modified gravity, taking the HSF into mind. As $t \longrightarrow 0$, the HSF deceleration parameter falls to $q \simeq -1 + \frac{1}{\mathcal{H}^1}$ and changes throughout cosmic time to become $q \simeq -1$ at the end of the culmination of cosmic evolution

The transit epoch correlates to a redshift called transit redshift z_a, which happens when the cosmos switches from a decelerated to an accelerated phase. This value has been constrained to be of the order of one based on several theoretical and empirical factors, i.e. $z_a \sim 1$. For instance, Busca [37] confined the redshift of the transition to be $z_a = 0.82 \pm 0.08$; and Capozziello et al. [38] succeeded in achieving a constraint on this parameter to be $z_a = 0.426^{+0.27}_{-0.089}$. According to Reiss et al. [39] calculated limitations of the transition redshift is $z_a = 0.69^{+0.23}_{-0.12}$. In contrast to Lu et al. [**?**] who got the constraint $z_a = 0.69^{+0.23}_{-0.12}$. The constraint was obtained by Moresco et al. [**?**] $z_a = 0.4 \pm 0.1$ .The deceleration parameter vanishes at the transit redshift, corresponding to a geological time $t = -\frac{\mathcal{H}^1}{\mathcal{H}^0} \pm \frac{\sqrt{\mathcal{H}^1}}{\mathcal{H}^0}$. One may have the transition period as $t = \frac{\sqrt{\mathcal{H}^1} - \mathcal{H}^1}{\mathcal{H}^0}$ in the context of orthodox Big Bang cosmology with a positive time frame only. It obviously limits the value of the parameter $\mathcal{H}^1$ to the range $0 < \mathcal{H}^1 < 1$. Mishra and Tripathy [31] have attempted to restrict this parameter to the range $0 < \mathcal{H}^1 < \frac{1}{3}$. $\mathcal{H}^0$ is treated as a free parameter in that work. In contrast, $\mathcal{H}^0$ is restricted in later work to the range $0.075 \leq \mathcal{H}^0 \leq 0.1$ in accordance with the restrictions on the transition redshift $0.4 \leq z_a \leq 0.8$ [34]. Additionally, Mishra et al. [32] replicated the transition redshift of $z_a = 0.806$ using the precise values $\mathcal{H}^0 = 0.695$ and $\mathcal{H}^1 = 0.085$. HSF is unquestionably necessary to reproduce the deceleration parameter's unique flipping behaviour. The value of $\mathcal{H}^0$, one of the two HSF parameters, determines how quickly a decelerating world transitions to an accelerating one. The pace of transition is faster the higher the value of $\mathcal{H}^0$. As a result, these parameters can be appropriately constrained using both the observed transit redshift values and the Hubble parameter data for various redshifts. In a recent study, we restricted the other parameters to achieve two specific values of the transition redshift, especially 0.8 and 0.5 [30] We also considered two specific values of $\mathcal{H}^1$, specifically 0.2 and 0.3. The purpose of doing this was to restrict the HSF's parameters.

It is undeniable that HSF is necessary to reproduce the deceleration parameter's hallmark flipping behaviour. The value of $\mathcal{H}^0$, one of the two HSF parameters, determines how quickly a decelerating world transitions to an accelerating one. The pace of transition is faster the higher the value of $\mathcal{H}^0$. As a result, these parameters can be appropriately limited using both the Hubble parameter data at various redshifts and the observed transit redshift values. In a recent study, we took into consideration three specific values of $\mathcal{H}^1$, particularly 0.1, 0.2 and 0.3 , and confined the other parameter to obtain the interval of transition redshift in between $0.4 < z_a \leq 0.9$. Six alternative models—Set1, Set2, Set3, Set4, Set5 and Set6—have been produced as a result of this approach. Table *I* lists the model parameters that were produced. The built-in models fall comfortably within the permitted bounds of the observed value.
TABLE I: Using transition redshift data from figure (5), constrain model parameters for the hybrid scale factor.

HSF Models	$\mathcal{H}^1$	$\mathcal{H}^0$	z_a
Set1	0.3	0.55	0.7
Set2	0.2	0.7	0.88
Set3	0.1	0.65	0.7
Set4	0.3	0.6	0.84
Set5	0.2	0.65	0.8
Set6	0.2	0.6	0.687

6. DISCUSSION OF BRANS-DICKE SCALAR FIELD

The Brans-Dicke scalar field is in this model is derived as,

$$\phi = \phi_0 \, t^{-3\mathcal{H}^1} e^{-3\mathcal{H}^0(t-1)} \left(\frac{\mathcal{H}^1}{t} + \mathcal{H}^0\right)^{-1}, \tag{40}$$

where the BD scalar field's value at the current epoch is ϕ_0, in this case. The scale factor's first derivative, together with both, affect the BD scalar field. The outcomes of Tripathy et al., [24] for an exponential and power law expansion of the scale factor can be retrieved from the BD scalar field calculation given above. The Hubble rate becomes constant for an exponential scale factor expansion, which causes the BD scalar field to be reduced to $\phi = \phi_0 a^3$.

Similar to how the BD scalar field changes with a power law expansion such as a $a \sim t^{\mathcal{H}^1}$, it becomes a $\phi \sim t^{3\mathcal{H}^1 - 1}$.

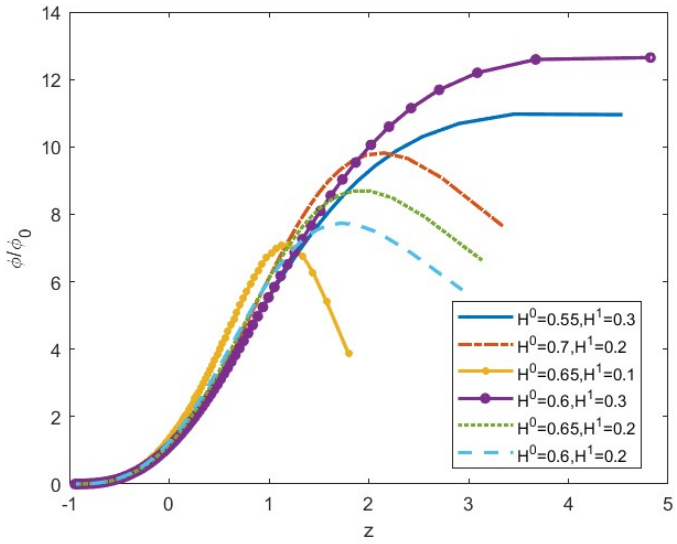

Figure 6. Evolution of the Brans-Dicke scalar field ϕ over the redshift z for six constraints.

The BD scalar field is shown in Fig:(6) for each model that has been constructed, transitioning from initially having some large values to currently having modest values. For the models with $\mathcal{H}^1 = 0.2$ and$\mathcal{H}^1 = 0.1$, however, ϕ first increases during the first phase to a specified maximum and subsequently decreases to the typical behaviour at a specific redshift. The HSF model performs the same at low redshift regardless the parameters of the model. Although behaves uniformly for all HSF models in the current epoch and those that follow, it's crucial to note that they exhibited fundamentally different behaviours at redshifts $z > 0.5$ during a prior cosmic phase. The behaviour of the models Set1 and Set4 appears to be smooth in terms of the development of the BD scalar field. Therefore, compared to the other four assumptions, these two approaches might be better suited for the cosmological study.

7. INVESTIGATION OF THE BRANS-DICKE PARAMETER

A prior work [24] used the built-in anisotropic models to compute the Brans-Dicke parameter while taking into consideration UDF within the context of the GBD theory and assuming either a power law or an exponential increase of the volume scale factor. The deceleration parameter is constant as a result of this assumption. It has been shown that in such cases the anisotropic parameter only influences the non-evolving part of the Bran-Dicke parameter. The hybrid expansion law we examined in this work, however, replicates the true transitory universe with early deceleration and late cosmic expansion.

The Brans-Dicke parameter is calculated in this work as,

$$\mathcal{W}(\phi) = \left[-3\frac{(\mathcal{H}^1+\mathcal{H}^0 t)}{t} + \frac{\mathcal{H}^1}{t(\mathcal{H}^1+\mathcal{H}^0 t)}\right]^{-2} \left\{ \begin{array}{l} \dfrac{8\pi c^1(\mathcal{H}^1+\mathcal{H}^0 t)}{t\,\phi_0\, t^{3\mathcal{H}^1\alpha}\, e^{3\mathcal{H}^0(\alpha t+1)}} - \dfrac{9(2n^2+3n+5)(\mathcal{H}^1+\mathcal{H}^0 t)^2}{(n+2)^2 t^2} \\ -2\left(\dfrac{\mathcal{H}^1}{t(\mathcal{H}^1+\mathcal{H}^0 t)}\right)^2 \end{array} \right\}, \tag{41}$$

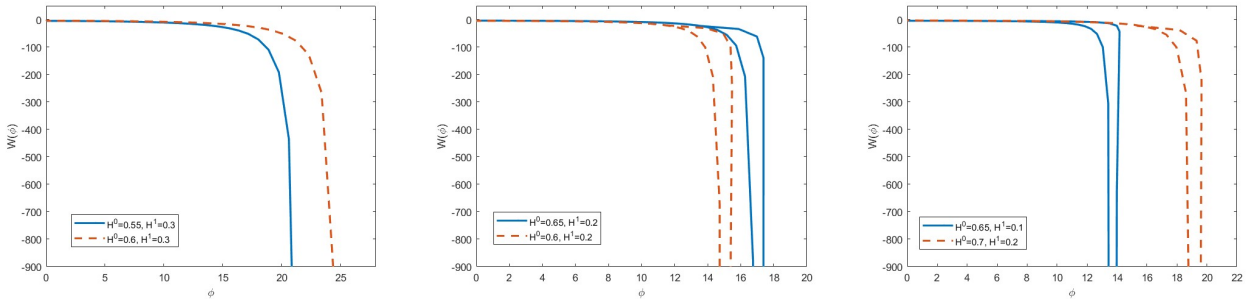

Figure 7. The Brans-Dicke parameter, $\mathcal{W}(\phi)$ for is shown over the scalar field ϕ for all $\mathcal{H}^0$ and $\mathcal{H}^1$ constraints.

Figures (7) (a), (b), and (c) show how the Brans-Dicke parameter has changed in relation to the BD scalar field . In each graph, the BD parameter is displayed for the two models. In Fig. (7)(a) $\mathcal{H}^0$ values are 0.55 and 0.6 with $\mathcal{H}^1 = 0.3$, in Fig. (7)(b) $\mathcal{H}^0$ values are 0.65 and 0.6 with $\mathcal{H}^1 = 0.2$, and in Fig. (7)(c) $\mathcal{H}^0$ values are 0.7 and 0.65 with $\mathcal{H}^1 = 0.2$ and 0.1 respectively. We took into account the value of α=0.0172 in order to visualise the data.

The BD parameter frequently falls as the scalar field gets larger. However, it is noted that at the late stages of cosmic history, behaves consistently across all models generating a kind of loop structure in the cases that we presented in Fig.(7)(a) when $\mathcal{H}^1 = 0.3$. For the cases with $\mathcal{H}^1 = 0.1$ and 0.2 in Fig.(7)(b) and 8(c), at some early epochs, $\mathcal{W}(\phi)$ exhibits strange behaviour, forming a type of loop structure with the scalar field. This tendency may be a result of the peculiar behaviour of the BD scalar field for the set2, set3, set5, and set6 models, which shows decrease with z, a minimum at a particular z, and then grows as z grows further. As a result, set1 and set4 may be more appropriate models for cosmological studies than the others. Notably, the BD parameter eventually becomes a constant value irrespective of the HSF parameters chosen at a later stage of cosmic evolution. The quantitative estimation of the BD parameter remains a contentious topic. However, our research revealed that all models anticipate values that are essentially the same. This leads to the conclusion that the anisotropy in the expansion rates influences the value at a certain epoch.

8. SELF–INTERACTING POTENTIAL

The self interacting potential $\mathcal{V}(\phi)$ in this model is calculated as,

$$\mathcal{V}(\phi) = \left[\frac{\phi_0}{t^{3\mathcal{H}^1} e^{3\mathcal{H}^0(t-1)\left(\frac{\mathcal{H}^1}{t}+\mathcal{H}^0\right)}}\right]\left\{\begin{array}{l}\frac{9(n^2+7n+2)}{(n+2)^2}\left(\frac{\mathcal{H}^1}{t}+\mathcal{H}^0\right)^2 \\ +\frac{2(\mathcal{H}^1)^2}{t^2(\mathcal{H}^1+\mathcal{H}^0 t)^2} \\ -\frac{3(n+5)\mathcal{H}^1}{t^2}-\frac{2\mathcal{H}^1}{t^2(\mathcal{H}^1+\mathcal{H}^0 t)}\end{array}\right\}+8\pi\left(\frac{2\alpha\rho_0}{(1+\alpha)}-\frac{c_2(1-\alpha)}{(1+\alpha)}\frac{1}{t^{3\mathcal{H}^1(1+\alpha)}e^{3\mathcal{H}^0 t(1+\alpha)}}\right), \tag{42}$$

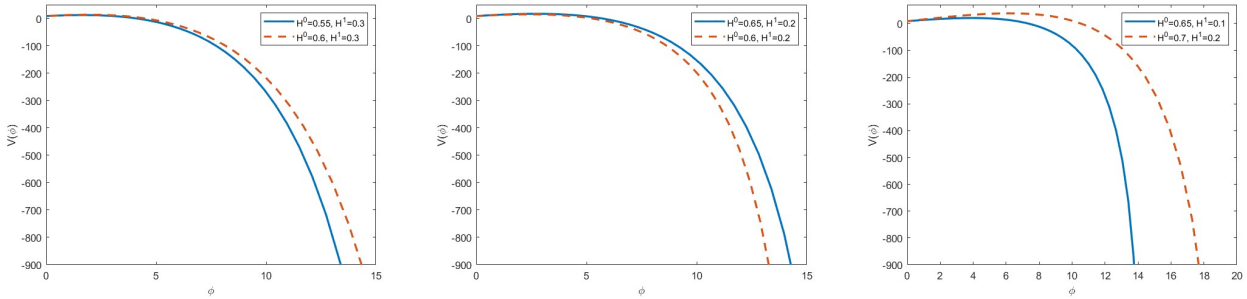

Figure 8. Study of the self interacting potential $\mathcal{V}(\phi)$ over the scalar field ϕ for all constraints of $\mathcal{H}^0$ and $\mathcal{H}^1$.

Figures 9(a), 9(b), and 9(c) show the self-interacting potential $\mathcal{V}(\phi)$'s variation as a function of the BD scalar field. For the two models in each graph, the self-interacting potential nature is displayed. In Fig.9(a) $\mathcal{H}^0$ values are 0.55 and 0.6 with $\mathcal{H}^1 = 0.3$, in Fig.9(b) $\mathcal{H}^0$ values are 0.65 and 0.6 with $\mathcal{H}^1 = 0.2$, and in Fig.9(c) $\mathcal{H}^0$ values are 0.7 and 0.65 with $\mathcal{H}^1 = 0.2$ and 0.1 respectively. We took into account the value of α=0.0172 to visualise the data.

The built-in HSF models have an attractive self-interacting potential that rises sharply from a significant negative value at an early epoch to virtually nothing at the end of evolution.The six models act in a manner that is comparable at the low redshift area, when the scalar field has a smaller magnitude. On the other hand, the six models split to act differently at the high redshift area with a big scalar field. At a late stage in the evolution of the universe, the self-interacting potential stops being reliant on HSF models and appears to be static about the BD scalar field.

9. NEWTONIAN GRAVITATIONAL CONSTANT G'S FLUCTUATION

The Newtonian gravitational constant $G(\phi)$ is described as follows in GBD theory:

$$G(\phi) = \frac{4+2\mathcal{W}(\phi)}{\phi(3+2\mathcal{W}(\phi))}, \tag{43}$$

so its variation of time is as

$$\frac{\dot{G}}{G} = \frac{-2\dot{\mathcal{W}}(\phi)}{(4+2\mathcal{W}(\phi))(3+2(\phi))} - \frac{\dot{\phi}}{\phi}. \tag{44}$$

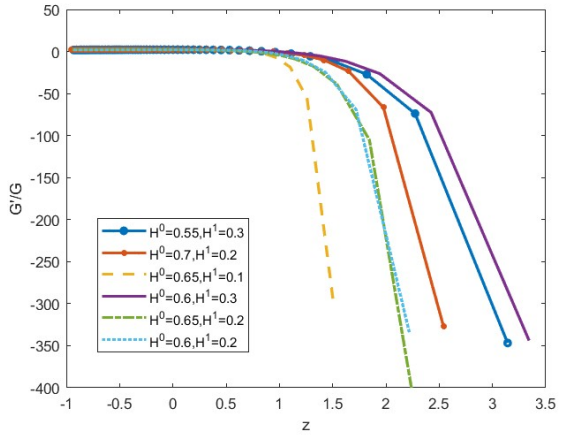

Figure 9. Study of $\frac{\dot{G}}{G}$ over the redshift z. Here we fixed the $\alpha = 0.0172$.

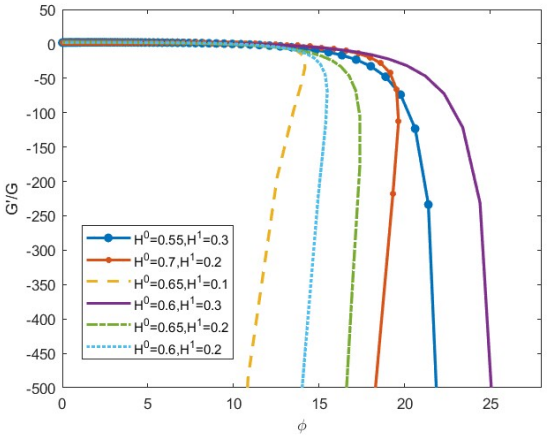

Figure 10. Study of $\frac{\dot{G}}{G}$ over the function ϕ. Here we fixed the $\alpha = 0.0172$.

In Figure (9) we display the G's time variation for the six HSF models as a function of redshift. We have shown the G time variation as a function of redshift. The determining $\frac{\dot{G}}{G}$ climbs from a previously significant negative value and reached a high in the recent past. It then drops to a somewhat positive number. The $\frac{\dot{G}}{G}$ peaks for various models occur at various redshifts. For a fitted model, the z_{max} at which $\frac{\dot{G}}{G}$ peaks is determined by the values of z_a and $\mathcal{H}^1$. For a specific $\mathcal{H}^1$, higher z_a causes higher z_{max}. Similar to this, larger $\mathcal{H}^1$ values translate into higher z_{max} for a given z_a. The temporal variation of the Newtonian gravitational constant as a result of the BD scalar field is also shown in Figure (10). It is noted that the factor $\frac{\dot{G}}{G}$ initially increases with an increase in and then decreases after peaking at a particular value for all six HSF models. The particular HSF models and associated model parameters determine which BD scalar field hosts the peak of $\frac{\dot{G}}{G}$.

10. CONCLUSION

The dynamics of our cosmos are incredibly complex, according to numerous observable pieces of evidence. The history of the universe's expansion is shown using a variety of methods because it is unknown exactly what these enigmatic fluids are in their most basic form. One of the most widely accepted theories postulates that dark energy and dark matter develop independently of one another, with the dynamics of each dark fluid existing independently of the other. Furthermore, it's believed that these two black fluids are just two sides of a single fluid, posing as both dark fluids. In cosmological literature, the idea of a single dark fluid that displays two distinct dark sides of the cosmos is referred to as the "unified dark fluid." In the current work, we have concentrated on a unified dark fluid model. Using GBD, we have developed a few astronomical models that accelerate. We pick Bianchi type$-VI_0$ directional expansion rates that are anisotropic and homogeneous in space. The GBD theory postulates that the Brans-Dicke parameter fluctuates with the scalar field. The Brans-Dicke hypothesis modifies the GR by proposing that gravity is propagated by a dynamic scalar field. The late-time cosmic speed-up phenomenon has been verified by observations. We employ a unified dark fluid equation of state that combines the treatment of dark matter and dark energy into a single equation, allowing us to build accelerated simulations. The parameters of the unified dark fluid model have been subject to limitations generated from various observational data using different techniques. Observational constraints have been used to establish the operational range of the model. construct a workable cosmological model inside the GBD hypothesis. The universe is expanding faster and faster. It suggests that, at some point in time, the universe may have entered an acceleration phase after experiencing a period of deceleration. The deceleration parameter, which should be positive at some early point in cosmic history and negative at some late point, must flip as a signature for this behaviour. We employ a hybrid scale factor to roughly represent a deceleration parameter with clear switching behaviour. Two components comprise the HSF. One element is more prevalent in the early phases of cosmic evolution than the other element is in the later stages. The HSF could thus recreate an entire journey history, beginning with an early deceleration and concluding with a late-time acceleration. The HSF's parameters must be restricted to provide a testable accelerated cosmological model. The transition redshift, which marks the potential turning point from a decelerating to an expanding universe, is a crucial cosmological statistic. To constrain the HSF parameters, we studied the recently constrained transition redshift values. In particular, we employed six transition redshift values in our work, ranging from $z_a = 0.65$ to $z_a = 0.9$. For an accelerated model, six distinct models are set up. We looked into the scalar field evolution, Brans-Dicke parameter, self-interacting potential, and time variation of the Newtonian gravitational constant for these models. For each of the constructed models, the BD scalar field changes with time from initially having some large values to later having smaller values. The BD scalar fields of all HSF models react identically at a late stage of evolution. For the models Set4 and Set6, however, the redshift first increases during the

first phase to a specific maximum before declining to the typical behaviour at a specific low redshift. For the BD scalar field, the evolutionary behaviour of the other four models is a little bit smoother. This behaviour is consistent with the evolution of other parameters, such as the BD parameter and the fluctuation of the Newtonian gravitational constant.The BD parameter decreases along with the BD scalar field, which increases in every model that has been built. Because the BD parameter virtually becomes a constant amount at a later stage of evolution, the GBD theory may be convergent with the standard Brans-Dicke theory. A major negative value at an early epoch diminishes to ridiculously small values later in development, making the self-interacting potential of the built-in HSF models desirable by nature. The models behave similarly when the scalar field has a smaller amount at low redshift. In the large redshift sector with a big scalar field, however, all models split to act differently.

11. ACKNOWLEDGMENTS

M. Vijaya Santhi acknowledges Department of Science and Technology (DST), Govt of India, New Delhi for financial support to carry out the Research Project [No. EEQ/2021/000737, Dt. 07/03/2022].

ORCID

M. Vijaya Santhi, https://orcid.org/0000-0002-0050-3033; **K. SantoshRupa**, https://orcid.org/0009-0001-8996-8661

REFERENCES

[1] A.G. Riess, *et al*., Astron J. **116**, 1009 (1998). https://doi.org/10.1086/300499

[2] S. Perlmutter, *et al*., Nature, **391**, 51 (1998). https://doi.org/10.1038/34124

[3] C.L. Bennett, *et al*., Astrophys. J. suppl. **148**, 1 (2003). https://doi.org/10.1086/377253

[4] D.N. Spergel, *et al*., Astrophys. J. Suppl. **148**, 175 (2003). https://doi.org/10.1086/377226

[5] S.M. Carroll, *et al*., Living. Rev. Relativ. **4**, 1 (2001). https://doi.org/10.12942/lrr-2001-1

[6] T. Padmanabhan, Phys. Rep. **380**, 235 (2003). https://doi.org/10.1016/S0370-1573(03)00120-0

[7] C.H. Brans, and R.H. Dicke, Phys. Rev. **124**, 925 (1961). https://doi.org/10.1103/PhysRev.124.925

[8] C.M. Will, *Theory and Experiment in Gravitational Physics*, (Cambridge University, Cambridge, (1981).

[9] C. Mathiazhagan and V.B. Johri, Class. Quantum Grav. **1**, L29 (1984). https://doi.org/10.1088/0264-9381/1/2/005

[10] D. La, and P.J. Steinhardt, Phys. Rev. Lett, **62**, 376 (1989). https://doi.org/10.1103/PhysRevLett.62.376

[11] N. Banerjee and D. Pavon, Class. Quant. Grav., 18, 593 (2001).

[12] S. Sen and A.A. Sen, Phys. Rev. D, 63, 124006 (2001).

[13] D.F. Mota and J.D. Barrow, Mon. Not. R. Astron. Soc. 349, 291 (2004).

[14] D.F. Mota and J.D. Barrow, Phys. Lett. B, 581, 141 (2004).

[15] S. Das and N. Banerjee, Phys. Rev. D, 78, 043512 (2008).

[16] N. Banerjee and D. Pavon, Phys. Rev. D, **63**, 043504 (2001). https://doi.org/10.1103/PhysRevD.63.043504

[17] K. Nordtvedt (Jr), Astrophys. J. **161**, 1059 (1970). https://doi.org/10.1086/150607

[18] J.P. Mimoso and A.M. Nunes, Phys. Lett A, **248**, 325 (1998). https://doi.org/10.1016/S0375-9601(98)00724-5

[19] M.V. Santhi, *et al*., Canadian Journal of Physics, **95**(2), 179 (2017). https://doi.org/10.1139/cjp-2016-0628

[20] E.A. Hegazy, and F. Rahaman, Indian Journal of Physics, **94**(11), 1847 (2020). https://doi.org/10.1007/s12648-019-01614-4

[21] Y. Aditya, *et al*., Indian Journal of Physics, 95, 383 (2021). https://doi.org/10.1007/s12648-020-01722-6

[22] D. Chhajed, *et al*., Journal of Ultra Scientist of Physical Sciences-Section A. (Mathematics), 34(4), (2022). http://dx.doi.org/10.22147/jusps-B/340401

[23] S.K. Tripathy, *et al*., Physics of the Dark Universe **30**, 100722 (2020). https://doi.org/10.1016/j.dark.2020.100722

[24] S.K. Tripathy, *et al*., The European Physical Journal C, **75**, 149 (2015). https://doi.org/10.1140/epjc/s10052-015-3371-3

[25] C.B. Collins, *et al*., Gen. Relativ. Gravit. **12**, 805, (1980). https://doi.org/10.1007/BF00763057

[26] S. Capozziello, *et al*., Phys. Rev. D, **73**, 043512 (2006), https://doi.org/10.1103/PhysRevD.73.043512

[27] E. Babichev, *et al*., Clas. Quant. Grav. **22**, 143 (2005). https://doi.org/10.1088/0264-9381/22/1/010

[28] S.K. Tripathy, *et al*., Physics of the Dark Universe, **30**, 100722 (2020). https://doi.org/10.1016/j.dark.2020.100722

[29] R.R. Caldwell, Phys. Lett. B, **545**, 23 (2002). https://doi.org/10.1016/S0370-2693(02)02589-3

[30] E.V. Linder, Phys. Rev. Lett. **90**, 091301 (2003). https://doi.org/10.1103/PhysRevLett.90.091301

[31] B. Mishra and S.K. Tripathy, Mod. Phys. Lett. A, **30**, 1550175 (2015). https://doi.org/10.1142/S0217732315501758

[32] B. Mishra, *et al*., Mod. Phys. Lett. A, **33**, 1850052 (2018). https://doi.org/10.1142/S0217732318500529

[33] B. Mishra, *et al*., Astrophys. Space Sci. **363**, 86 (2018). https://doi.org/10.1007/s10509-018-3313-2

[34] P.P. Ray, *et al*., Int. J. Mod. Phys. D, **28**, 1950093 (2019). https://doi.org/10.1142/S0218271819500937

[35] B. Mishra, *et al*., Mod. Phys. Lett. A, **34**, 1950217 (2019). https://doi.org/10.1142/S0217732319502171

[36] B. Mishra, *et al*., Journal of Astrophysics and Astronomy, **42**, 2 (2021). https://doi.org/10.1007/s12036-020-09655-6

[37] N.G. Busca, Astron. Astrophys. 552, A96 (2013). https://doi.org/10.1051/0004-6361/201220724

[38] S. Capozziello, *et al*., (2014). https://doi.org/10.48550/arXiv.1403.1421

[39] A.G. Reiss, *et al*., Astrophys. J. **659**, 98 (2007). https://doi.org/10.1086/510378

[40] J. Lu, *et al*., Phys. Lett. B, **699**, 246 (2011). https://doi.org/10.1016/j.physletb.2011.04.022

[41] M. Moresco, *et al*., (2016). https://doi.org/10.48550/arXiv.1601.01701

ДОСЛІДЖЕННЯ КОСМОЛОГІЧНИХ МОДЕЛЕЙ АНІЗОТРОПНОЇ ТЕМНОЇ ЕНЕРГІЇ В УЗАГАЛЬНЕНІЙ ТЕОРІЇ БРАНСА-ДІКЕ

М. Віджая Санті, **К. СантошРупа**

Факультет прикладної математики, Університет Андхра, Вісакхапатнам 530003, Індія

У цій статті ми досліджували космологічну модель темної енергії в просторі-часі Б'янчі–VI_0, розглядаючи узагальнену теорію Бранса-Дікке, потенціал самовзаємодії та параметр динамічного зв'язку. Для цієї мети ми використали гібридний масштабний коефіцієнт для наближення динамічної поведінки параметра уповільнення. Параметр уповільнення повинен демонструвати характерну поведінку перевертання при перехідному червоному зсуві, оскільки вважається, що Всесвіт змінився з раннього уповільнення на пізнє часове прискорення. Ми вивчили шість альтернативних моделей переходу темної енергії на основі спостережних обмежень на червоне зміщення переходу. Для кожної моделі досліджено поведінку динамічного скалярного поля, параметра Бранса-Дікке та потенціалу самовзаємодії. Крім того, ми використали узагальнену теорію Бранса-Дікке, щоб оцінити, як ньютонівська гравітаційна стала змінюється з часом.

Ключові слова: *метрика типу Б'янчі–VI_0; узагальнена теорія Бранса-Дікке; гібридний масштабний коефіцієнт; параметр асиметрії; уніфікована темна рідина*